

# Hollow-core microstructured ‘revolver’ fibre for the UV spectral range

A.D. Pryamikov, A.F. Kosolapov, G.K. Alagashev,  
A.N. Kolyadin, V.V. Vel’miskin, A.S. Biriukov, I.A. Bufetov

**Abstract.** We report the first silica-based hollow-core microstructured fibre for the UV spectral range, with a reflective cladding formed by a single ring of capillaries. The optical loss in the fibre at a wavelength of 250 nm is 3 dB m<sup>-1</sup>. We demonstrate distinctions between the propagation of high-order modes and the fundamental mode of the hollow core of a ‘revolver’ fibre with noncontacting cladding capillaries and examine the effect of multimode excitation on the transmission bandwidth of the fibre. Based on experimental data and numerical simulation results, we formulate recommendations how to reduce the level of losses and extend transmission bands in a hollow-core revolver fibre in the UV spectral range.

**Keywords:** hollow-core fibre, microstructured fibre.

## 1. Introduction

‘Revolver’ fibres (RFs) are a class of microstructured fibres that allow electromagnetic radiation to propagate in their gas-filled hollow core. There are currently several main types of hollow-core microstructured fibre (HCMF), in which the light localisation mechanism is determined by the optical properties of their microstructured cladding [1–3]. The term ‘localisation’ is here taken to mean mode field confinement in the hollow core. Effective light localisation in the HCMF core is due to the constructive interference of the propagating light when it is reflected from microstructured cladding elements. Various physical mechanisms can be responsible for the localisation. Currently, the best known and best studied mechanism is light localisation based on photonic bandgaps in photonic-crystal fibres (PCFs) [1]. This mechanism is operative, for example, in HCMFs with a two-dimensional hexagonal photonic-crystal cladding. The degree of light localisation (the percentage of light propagating in the core) in such microstructures in the near-IR region can be very high [4]. The linear dimensions of the main elements in the structure of the HCMF cladding are proportional to the wavelength of light. Because of this, HCMFs for the UV region are more difficult to fabricate, which limits their potential applications. The shortest wavelength transmission band obtained in such HCMFs lies around  $\lambda = 850$  nm [5]. One type of hollow-core fibre is fibre with a Kagome lattice microstructured cladding

[2]. Such a cladding has a low spectral density of eigenmodes, and the modes of the hollow core are weakly coupled to them (small overlap integral) because their spatial distributions differ drastically. For this reason, the transmission bandwidth of such fibres considerably exceeds that of PCFs. At the same time, losses in the HCMFs with a Kagome lattice cladding are considerably higher than those in the PCFs [2]. This and the fact that Kagome lattice claddings are more difficult to reproduce and fabricate at shorter wavelengths also impede the use of such fibres in the UV region.

Recently demonstrated silica HCMFs with a negative curvature of their core–cladding boundary are a new type of hollow-core fibre that allows for electromagnetic radiation transmission in the mid- to near-IR spectral region [6–8]. Note that the transmission bandwidth of such HCMFs exceeds that of the PCFs and their fundamental air-core modes have a considerably higher degree of localisation. The cladding of the HCMFs with a negative curvature of their core–cladding boundary has a much simpler structure than does that of the HCMFs considered above. For example, the cladding of a revolver fibre is formed by a single ring of capillaries located on the inner surface of a substrate tube [6, 8].

In this paper, we examine the possibility of transmitting UV light through revolver HCMFs. The ability to produce such waveguides is of key importance for many applications in medicine, lithography, photochemistry and sensing technology [9–12].

All-glass fibres are ineffective in UV light transmission because the material optical loss in such fibres rapidly increases with decreasing wavelength. The air in the HCMF core has a much broader transmission window than does silica glass (but with Schumann–Runge absorption bands [13]). Because of this, hollow-core fibres are among the most attractive candidates for use as a waveguiding structure for light transmission in a wide wavelength range (exceeding the transmission window of silica glass).

Figure 1 shows measured losses in the different types of HCMF described above. It is seen that, even with the current, imperfect technology, HCMFs made of silica glass have good guidance properties in the mid-IR region. Light at wavelengths of up to  $\lambda = 8000$  nm was transmitted using HCMFs with a negative curvature of their core–cladding boundary [Fig. 1, curve (4)]. Note that it is RFs that ensured waveguiding in the spectral range where silica glass has high losses. Near  $\lambda = 3000$  nm, RFs [point (5)] and HCMFs with parachute-shaped cladding elements [points (8)] have roughly equal losses (30–50 dB km<sup>-1</sup>). Near  $\lambda = 1500$  nm, photonic bandgap-based HCMFs have the lowest measured loss [points (6)]. Much less data have been reported on the char-

A.D. Pryamikov, A.F. Kosolapov, G.K. Alagashev, A.N. Kolyadin,  
V.V. Vel’miskin, A.S. Biriukov, I.A. Bufetov Fiber Optics Research  
Center, Russian Academy of Sciences, ul. Vavilova 38, 119333  
Moscow, Russia; e-mail: pryamikov@fo.gpi.ru

Received 30 September 2016; revision received 22 October 2016  
*Kvantovaya Elektronika* 46 (12) 1129–1133 (2016)  
Translated by O.M. Tsarev

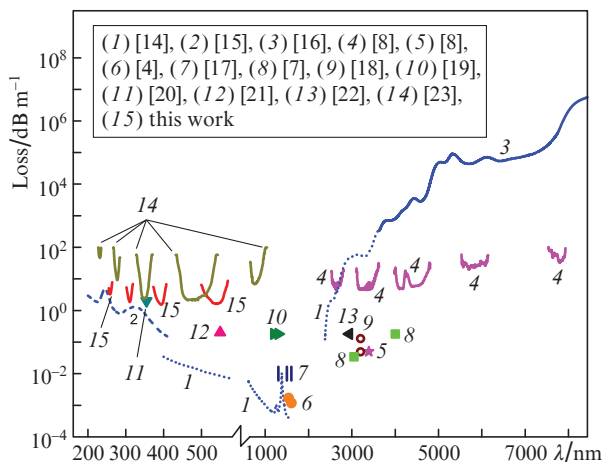


**Figure 1.** (1–3) Optical losses in pure silica glass (F300, Heraeus) and (4–15) minimum optical losses obtained to date in various types of silica-based HCMF.

acteristics of hollow-core microstructured fibres in the UV region [point (11), curves (14)].

In this paper, we examine the feasibility of UV light transmission through hollow-core RFs. To this end, we have fabricated a specially designed silica fibre intended for UV light transmission (RF1) and measured its optical losses in the visible and UV ranges. Due to some specific features of the fibre fabrication process, the geometric dimensions of RF1 vary along its length (with a spread of several percent). With the aim of further improving the fibre design and analysing mechanisms that influence the guidance properties of fibres, we performed mathematical modelling of light propagation through an idealised fibre with cross-sectional parameters obtained by averaging parameters measured in different cross sections of RF1. The modelling results were compared to experimental data.

## 2. Optical fibre

The key parameters determining light propagation through RFs include the ratio of the wavelength  $\lambda$  of the light to the core diameter  $D_{\text{core}}$  ( $\lambda/D_{\text{core}}$ ) and the ratio of the thickness  $t$  of the capillary wall in the fibre cladding to the wavelength ( $t/\lambda$ ). As shown earlier [8], an RF having a reflective cladding formed by eight capillaries,  $D_{\text{core}} = 119 \mu\text{m}$  and  $t = 6 \mu\text{m}$  offers a satisfactory performance in the wavelength range  $\lambda = 2000\text{--}8000 \text{ nm}$ . Therefore, in the range  $\lambda = 200\text{--}500 \text{ nm}$  (about one order of magnitude shorter wavelengths) use should be made of fibre having an order of magnitude smaller core diameter and capillary wall thickness. Such fibre was fabricated in this study. Its cross section is presented in Fig. 2. The fibre fabrication process was similar to that described elsewhere [8, 24]. The capillary wall thickness was 590–630 nm and the core diameter was 15  $\mu\text{m}$ . To ensure the possibility of handling the fibre (impart to it appropriate mechanical properties), the thickness of its outer silica tube was increased so that its outer diameter after fibre drawing exceeded 70  $\mu\text{m}$  (it was determined to be 73  $\mu\text{m}$ ).

The optical loss spectrum of the RF1 fibre [Fig. 3, curve (1)] was measured by the cut-back technique. We used RF1 segments shorter than 1 m, and the light source used was an Ocean Optics DH-2000 deuterium lamp. Its light was coupled

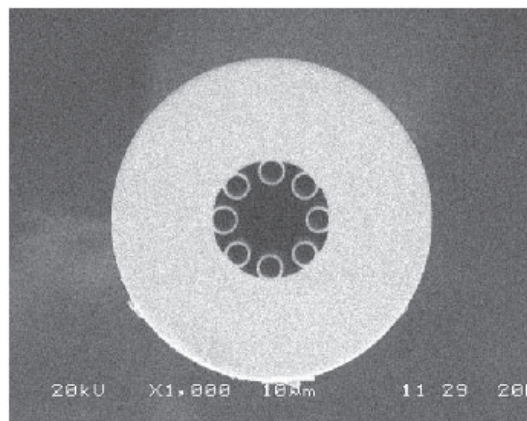


**Figure 2.** Cross-sectional SEM image of the RF1 fibre (outer diameter, 73  $\mu\text{m}$ ).

into RF1 using a lens. The optical loss spectrum thus obtained in the wavelength range 250–600 nm demonstrates that this range contains four transmission bands, with minimum losses of 3.25, 1.9, 1.55 and 1.62  $\text{dB m}^{-1}$  at  $\lambda = 258, 310, 393$  and 540 nm, respectively. It is seen in Fig. 1 that, in the visible range, the loss in RF1 substantially exceeds that in pure silica glass. At the same time, silica glass and RF1 have comparable losses in the UV region (near  $\lambda = 250 \text{ nm}$ ).

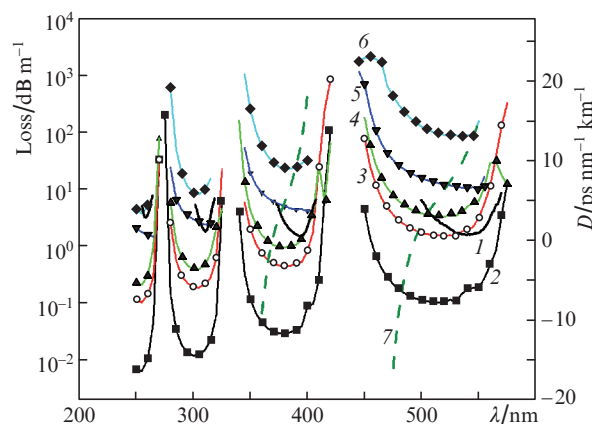


**Figure 3.** Measured optical loss spectrum of RF1 (1), calculated total loss for the fundamental (2) and high-order (3–6) air-core modes of an idealised HCMF and calculated group velocity dispersion  $D$  as a function of wavelength for RF1 (7).

Given that the measured dispersion in the RF agrees well with calculation results [25], here we restrict ourselves to calculating dispersion as a function of wavelength for the RF1 fibre [Fig. 3, curve (7)]. The RF1 fibre has low dispersion, which slightly exceeds 5  $\text{ps nm}^{-1} \text{ km}^{-1}$  in the middle of the transmission bands. Taking into account the low nonlinearity level of RFs (the mass density of the HCMF core is about three orders of magnitude lower than that of solids), the low dispersion in the RFs and their inherent stability to UV and ionising radiation exposure, it is already clear that the RFs have a number of advantages over pure silica fibres for applications in the UV region.

### 3. Analysis of the spectral dependences of the total loss in revolver HCMFs in the UV spectral range

For the numerical simulation and analysis of spectral dependences of losses in RF1 (Fig. 2), we used an idealised fibre having a similar geometric structure. Its characteristic dimensions were as follows: hollow-core diameter  $D_{\text{core}} = 15 \mu\text{m}$ , capillary wall thickness  $t = 0.62 \mu\text{m}$  and inner capillary diameter  $d = 4.36 \mu\text{m}$ . Loss calculation for the fundamental mode of the hollow core showed that there was good agreement between the calculated and measured positions of the long-wavelength edges of the transmission bands of the HCMF under consideration [Fig. 3, curve (2)]. Comparison of experimental data and calculation results demonstrates a significant discrepancy between the positions of the short-wavelength edges of the experimentally measured transmission bands and the short-wavelength edges of the calculated transmission bands for the fundamental air-core mode (Fig. 3). In addition, the calculated position of the optical loss minimum for higher order modes in each transmission band is shifted to longer wavelengths from the centre of the band. Moreover, there is a significant discrepancy between the calculated total loss for the fundamental mode and the experimentally measured loss. Comparison of the experimental data and calculation results suggests some evidence that, under the experimental conditions of this study, not only the fundamental mode but also a few higher order modes were excited in short ( $\sim 1 \text{ m}$ ) pieces of the fibre. Note that the measured level of optical losses corresponds to some average value for a few excited modes and that the shift of the measured position of the absorption minimum in each transmission band to longer wavelengths corresponds to the analogous shift in the optical loss spectra of higher order modes in the RF1 fibre.

It is known that revolver HCMFs are currently classed with hollow-core antiresonant fibres [26, 27]. Light localisation in such fibres is due to the effective antiresonant reflection of the light propagating through their hollow core from cladding elements, in particular from the capillary walls in our case. If the resonance condition is met at a given wavelength,  $k_{\text{t}}t = \pi m$  [where  $k_{\text{t}} = \sqrt{k^2 - \beta^2}$  is the magnitude of the transverse wave vector;  $k$  is the magnitude of the wave vector of the light in the medium (air or glass);  $\beta$  is the mode propagation constant of the hollow core; and  $m$  is an integer], the loss rises sharply, and this determines the edge of the transmission band of the fibre. It is seen in Fig. 3 that this is indeed so for the fundamental and the first few modes of the hollow core. At the same time, the short-wavelength edge of the transmission bands of several higher order modes is shifted. The higher the hollow core mode number, the larger is the shift of the short-wavelength edge of the corresponding transmission band with respect to the wavelength that determines resonance in the capillary wall.

Multimode light propagation through the hollow core (with a relatively small difference in loss between the modes) is observed in HCMFs of the RF1 type, which have some spacing between the capillaries [28]. Waveguiding loss calculation for an HCMF having a cladding formed by eight contacting capillaries with the same wall thickness as above and having the same hollow-core diameter indicates (Fig. 4a) that in this case light propagates in the few-mode regime (the difference in optical loss between the modes is considerably larger). Note that, as the spacing between the capillaries in cross sections of fibres similar to that shown in Fig. 2

is continuously reduced to zero, the optical loss spectra of the fibres transform, also continuously, from those presented in Fig. 3 to the loss spectra in Fig. 4a. In the case of the RF design under consideration, purely single-mode light propagation appears to be difficult to ensure, because the loss for the fundamental mode of the hollow core, even though being lower than that for the first higher order mode (of the LP<sub>11</sub> type), is always comparable to it and differs from it by only a few times (as distinct from the losses for higher order modes).

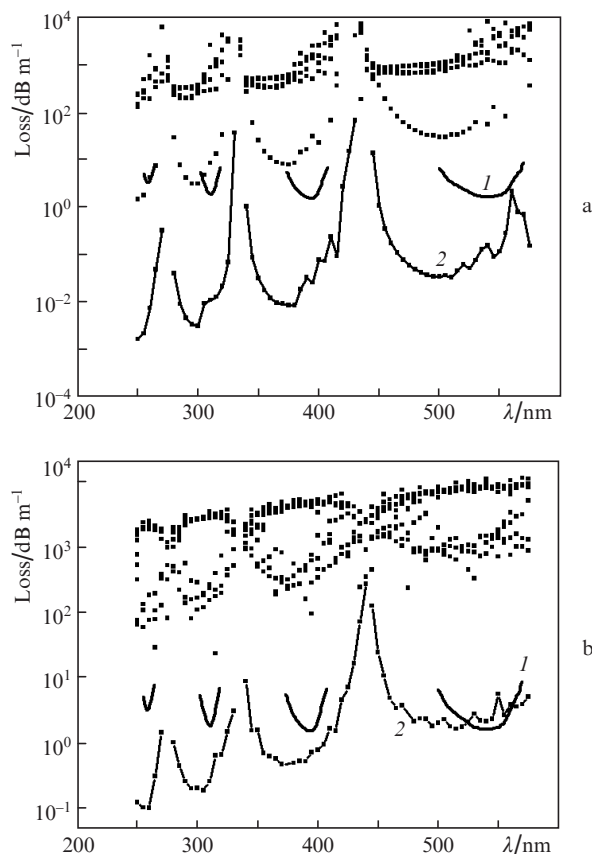


**Figure 4.** Spectral dependences of the waveguiding loss for air-core modes (a) in a revolver HCMF with contacting cladding capillaries and (b) in a waveguide with an octagonal cross section and the same thickness of the core–cladding boundary as above: (1) experimentally measured loss; (2) loss for the fundamental mode. The solid squares represent the loss for the higher order modes.

Figure 4b shows spectral dependences of the loss for modes of the hollow core of a waveguide with an octagonal core–cladding boundary (with no negative curvature). The thickness of the core–cladding boundary and the effective fundamental mode field area in the hollow core were the same as in the idealised HCMF with a cladding formed by noncontacting capillaries. The fundamental air-core modes in the HCMF with contacting cladding capillaries and in the octagonal microstructure differ in the level of losses (Fig. 4). The loss spectrum of the fundamental mode of the octagonal waveguide has a resonance nature owing to the excitation of core–cladding boundary modes with large azimuthal numbers [29]. Nevertheless, in both cases we observe light propagation through the hollow core in the few-mode regime. The higher order modes are strongly coupled to hollow-core

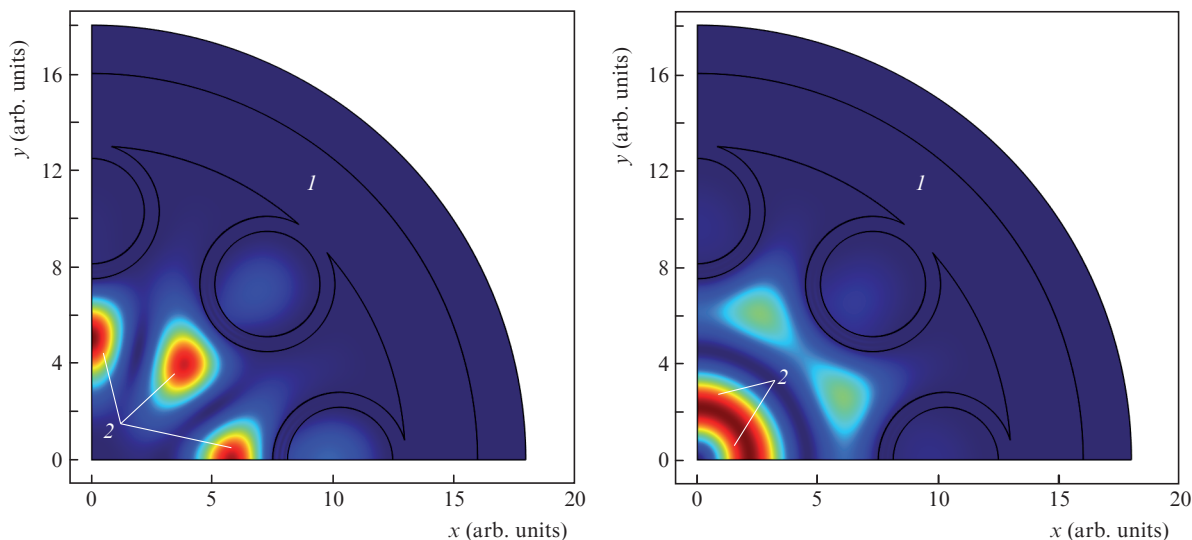


**Figure 5.** (Colour online) Energy flux density distributions at a wavelength  $\lambda = 475$  nm (Fig. 3) for two high-order air-core modes of the hollow core in an idealised revolver HCMF. The dark blue colour [regions (1)] corresponds to zero optical field; the red colour [regions (2)], to the maximum field; and the intermediate hues, to intermediate field intensities.

core–cladding boundary modes and are very leaky. This suggests that the mechanism of high-order mode localisation in the HCMF having eight contacting cladding capillaries is similar to that in the octagonal waveguide. We believe that this is due to the effective coupling between core–cladding boundary modes with a particular type of rotational symmetry and high-order air-core modes [28].

It is also seen in Fig. 4 that, in the cases under consideration, there is no shift of the short-wavelength edge of the transmission bands for the high-order modes of the hollow core. It is therefore reasonable to conclude that the main contribution to the increase in the number of high-order modes in the HCMF (Fig. 2) is made by the free spaces between the capillaries. As distinct from the fundamental air-core mode, the light of high-order modes penetrates the spaces between the capillaries, thereby increasing the effective area of the interaction of the light with the capillary wall and the holes in the capillaries. In contrast to the revolver HCMF with contacting cladding capillaries, in this case there is no interaction of air-core modes with modes of the core–cladding boundary as a whole, and each capillary can be thought of as an individual scatterer. As a result, there is no effective coupling of the core–cladding boundary modes to the high-order air-core modes.

Figure 5 presents examples of energy flux density distributions across an idealised HCMF for two high-order modes. Since the shift of the short-wavelength edge of the transmission band for these air-core modes cannot be related to resonance in the capillary wall, there is resonance light leakage to the holes of the capillaries and the spaces between them.

Thus, higher order mode excitation in short pieces of a revolver HCMF (Fig. 2) in the UV spectral range leads to a high level of total measurable losses and a reduction in the transmission bandwidth of the HCMF. It seems likely that, if excitation of only the fundamental mode in the RF1 fibre were ensured, the measured optical loss would be related to only the fundamental mode and, hence, would be lower. In our case, the measured optical loss in the RF1 fibre can be thought of as the upper boundary of the optical loss for the fundamental mode. It is worth noting, however, that high

measured losses may also originate from a longitudinal non-uniformity in the geometric parameters of the fibre, which was left out of consideration in the mathematical modelling in this study.

## 4. Conclusions

A hollow-core revolver fibre having transmission bands in the UV spectral range and losses of the order of a few decibels per metre has been studied for the first time. The measured losses and transmission bandwidths were determined by specific features of the loss spectra for some of the high-order air-core modes. Nearly single-mode light propagation in the RF, with increased optical losses for the high-order modes in comparison with the fundamental mode, can be ensured by optimising the spacing between the cladding capillaries or varying the number of capillaries. We believe that, with improvements in the RF fabrication process, revolver HCMFs may have great potential for use in the UV spectral range.

**Acknowledgements.** This work was supported by the Russian Foundation for Basic Research (Grant No. 14-29-07176-ofi-m).

## References

1. Russell P.St.J. *J. Lightwave Technol.*, **24** (12), 4729 (2006).
2. Benabid F. *Philos. Trans. R. Soc. London, Ser. A*, **364**, 3439 (2012).
3. Russell P.St.J., Hölzer P., Chang W., Abdolvand A., Travers J.C. *Nat. Photonics*, **8**, 278 (2014).
4. Roberts P.J., Couny F., Sabert H., Mangan B.J., Williams D.P., Farr L., Mason M.W., Tomlinson A., Birks T.A., Knight J.C., Russell P.St.J. *Opt. Express*, **13** (1), 236 (2005).
5. Bouwmans G., Luan F., Knight J.C., Russell P.St.J., Farr L., Mangan B.J., Sabert H. *Opt. Express*, **11** (14), 1613 (2003).
6. Pryamikov A.D., Biriukov A.S., Kosolapov A.F., Plotnichenko V.G., Semjonov S.L., Dianov E.M. *Opt. Express*, **19** (2), 1441 (2011).
7. Yu F., Wadsworth W.J., Knight J.C. *Opt. Express*, **20** (10), 11153 (2012).
8. Kolyadin A.N., Kosolapov A.F., Pryamikov A.D., Biriukov A.S., Plotnichenko V.G., Dianov E.M. *Opt. Express*, **21** (8), 9514 (2013).

9. Jaryaraman V., Rodgers K.R., Mukerji I., Spiro T.G. *Science*, **269** (5232), 1843 (1995).
10. Cubillas A.M., Unterkofler S., Euser T.G., Etzold B.J.M., Jones A.C., Sadler P.J., Wasserscheid P., Russell P.St.J. *Chem. Soc. Rev.*, **42** (22), 8629 (2013).
11. Leggett G.J. *Nanoscale*, **4** (6), 1840 (2012).
12. Hanlon E.B., Manoharan R., Koo T.W., Shafer K.E., Motz J.T., Fitzmaurice M., Kramer J.R., Itzkan I., Dasari R.R., Feld M.S. *Phys. Med. Biol.*, **45** (2), R1 (2000).
13. El'yashevich M.A. *Atomnaya i molekulyarnaya spektroskopiya* (Atomic and Molecular Spectroscopy) (Moscow: Editorial URSS, 2001).
14. Humbach O., Fabian H., Grzesik U., Haken U., Heitmann W. *J. Non-Cryst. Solids*, **203**, 19 (1996).
15. Tomashuk A.L., Golant K.M. *Proc. SPIE Int. Soc. Opt. Eng.*, **4083**, 188 (2000).
16. Kryukova E.B., Plotnichenko V.G., Dianov E.M. *Proc. SPIE Int. Soc. Opt. Eng.*, **4083**, 71 (2000).
17. OFS; <http://fiber-optic-catalog.ofsoptics.com/asset/Hollow-Core-Optical-Fibers.pdf>.
18. Sandoghchi S.R., Poletti F., Petrovich M.N., Richardson D.J. *Opt. Lett.*, **39**, 295 (2014).
19. Wang Y.Y., Wheeler N.V., Couny F., Roberts P.J., Benabid F. *Opt. Lett.*, **36**, 669 (2011).
20. Février S., Beaudou B., Viale P. *Opt. Express*, **18**, 5142 (2010).
21. G r me F., Jamier R., Auguste J.-L., Humbert G., Blondy J.-M. *Opt. Lett.*, **35**, 1157 (2010).
22. Ulrich A., Maier R.R.J., Yu F., Knight J.C., Hand D.P., Shephard J.D. *Biomed. Opt. Express*, **4**, 193 (2013).
23. Hartung A., Kobelke J., Schwuchow A., Wondraczek K., Bierlich J., Popp J., Frosch T., Schmidt M.A. *Opt. Express*, **22**, 19131 (2014).
24. Kosolapov A.F., Alagashv G.K., Kolyadin A.N., Pryamikov A.D., Biryukov A.S., Bufetov I.A., Dianov E.M. *Kvantovaya Elektron.*, **46**, 267 (2016) [*Quantum Electron.*, **46**, 267 (2016)].
25. Kolyadin A.N., Alagashv G.K., Pryamikov A.D., Mouradian L., Zeytunyan A., Toneyan H., Kosolapov A.F., Bufetov I.A. *Phys. Procedia*, **73**, 59 (2015).
26. Litchinitser N.M., Abeeluck A.K., Headley C., Eggleton B.J. *Opt. Lett.*, **27** (18), 1592 (2002).
27. Yu F., Knight J.C. *IEEE J. Sel. Top. Quantum Electron.*, **22** (2), 4400610 (2016).
28. Alagashv G.K., Pryamikov A.D., Kosolapov A.F., Kolyadin A.N., Lukovkin A.Yu., Biriukov A.S. *Laser Phys.*, **25**, 055101 (2015).
29. Vincetti L., Setti V. *Opt. Express*, **20** (13), 14350 (2012).